Available on CMS information server **CMS NOTE 1998/046**

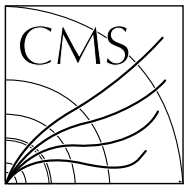


**The Compact Muon Solenoid Experiment**

# CMS Note

Mailing address: CMS CERN, CH-1211 GENEVA 23, Switzerland

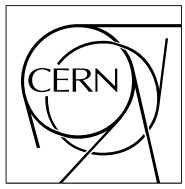


**July 1998**

# Pion damage in semiconductor lasers

K. Gill, V. Arbet-Engels, G. Cervelli, R. Grabit, C. Mommaert, G. Stefanini, F. Vasey

*CERN EP Division, CH-1211, Genève 23, Switzerland.*

J. Troska

*Blackett Laboratory, Imperial College, London SW7 2BZ.*

**Abstract**

Fully packaged, edge-emitting 1310nm wavelength semiconductor lasers, for use in CMS Tracker optical links, have been irradiated at room temperature with 330MeV positive pions. Measurements of the threshold current and slope-efficiency were made in-situ for pion fluences up to $5.2 \times 10^{14}$ $\pi^{+}/cm^{2}$. A comparison is made between pion damage and neutron, proton and gamma damage in terms of the threshold current increase in the lasers. 330MeV pions are 1.2 times more damaging than ($E_p$=24GeV) protons and 3.8 times more damaging than ($<E_n>$=6MeV) neutrons; gamma damage is negligible in comparison to hadron damage. Around 40% of the pion damage anneals in 600 hours at room temperature following irradiation. Higher temperature annealing steps (300 hours at 40, 60 and 80°C) recover a further 25% of the damage, with no anti-annealing.

# 1. Introduction

An analogue optical link is being developed at CERN for readout of the CMS tracking detectors[1-3]. One important aspect of this development is testing the radiation hardness of candidate link components for use inside the CMS Tracker. Over the first 10 years of LHC operation (or $10^5 pb^{-1}$ integrated luminosity), materials inside the Tracker will be exposed to integrated particle fluences[4] of ~$10^{14}$(1MeV neutrons)/$cm^2$, ~$1.6x10^{14}$ charged hadrons/$cm^2$ (80% pions, 10% protons, 10% kaons with energies in the range of several hundred MeV), plus a total ionising dose of ~100kGy. These figures are given, for example, for a distance of 22cm from the beam axis in the barrel part of the tracker, corresponding to the inner barrel layer of silicon strips. The particle fluences are significantly higher in the pixel layers, also dominated by pions with several hundred MeV energy, and lower in the MSGC layers, where ~1MeV neutrons become more important than charged hadrons.

The main effects of radiation damage observed in lasers are an increase in the threshold current, above which the stimulated emission dominates the light output, and a decrease in output efficiency - the increase in optical power output per unit of input current (above threshold). Radiation damage introduces defects into the crystal which can act as non-radiative recombination centres[5]. The presence of these defects in the active region of the laser causes the threshold current to increase as a result of having to compensate for the injected charge that is lost through non-radiative transitions. A loss of output efficiency can also occur at high fluences when the non-radiative recombination lifetime $\tau_{nr}$ decreases to a comparable level to that of the (stimulated) recombination lifetime $\tau_{st}$ of the carriers, since the efficiency E is related to the lifetimes by[6],

$$E = \frac{\frac{1}{\tau_{st}}}{\frac{1}{\tau_{st}} + \frac{1}{\tau_{nr}}} = \frac{\tau_{nr}}{\tau_{st} + \tau_{nr}} \quad (1)$$

and the non-radiative lifetime typically decreases with radiation fluence following the formula[6],

$$\frac{1}{\tau_{nr}} = \frac{1}{\tau_{nr}(0)} + K\Phi \quad (2)$$

if the defects are introduced linearly with fluence. The factor K is defined as the ‘damage constant’, which is sensitive to many factors such as material, type of radiation, particle energy, flux, and device temperature and electrical bias conditions. (We will avoid calculating the damage constant in this report due to its strong dependence on many factors which have not all been investigated in sufficient detail.)

An extensive study of radiation damage in lasers and other link components including p-i-n photodiode receivers and passive link components such as fibres and connectors is in progress[7-12]. Our focus has been mainly on InGaAsP multi-quantum-well (MQW), edge-emitting 1310nm lasers, in line with recent developments in the telecommunications market, but other lasers including VCSEL’s and edge-emitters at shorter wavelengths have also been tested. Approximately 100 lasers, from 8 manufacturers, have been irradiated with ~6MeV neutrons, with fluences of $10^{14}$-$10^{15}$n/$cm^2$ along with $^{60}$Co gamma irradiation up to 100kGy (10Mrad) on 15 lasers from 5 manufacturers (identical to devices irradiated with neutrons). Both fully

packaged devices and naked die were irradiated in earlier neutron and gamma tests with no significant difference in the damage effects.

In addition to neutron and gamma irradiation, a test with high energy charged hadrons (24GeV protons) was also carried out on NEC lasers, packaged and supplied by Italtel[a] (identical to some samples irradiated with neutrons and gammas) at the CERN PS beamline[8]. 24GeV protons caused approximately 3 times more damage than ~6MeV neutrons in terms of threshold increase and efficiency loss in the irradiated lasers (after corrections for annealing during irradiation are taken into account, as in Section 4). The increased damage from protons is likely to be related to the energy rather than the charge of the protons, since the extra ionisation damage during proton irradiation is not expected to be significant. A similar large difference is observed in irradiated GaAs detectors[13], with more damage after 24GeV proton irradiation compared to the same fluence of 1MeV neutrons, whereas in silicon detectors[14] the levels of damage are similar. This effect can be explained in terms of the non-ionising energy loss (NIEL)[15], which is hypothesised to be proportional to the amount of displacement damage produced by different incident particles (see Appendix).

In GaAs devices irradiated with 330MeV pions, 20% more damage occured than for the same fluence of 24GeV protons[13]. As pions will dominate the high energy particle fluence inside the CMS tracker at low radii, and given the similarity between the lasers and GaAs, pion damage (for energies around several hundred MeV) was clearly one of the most important unknown factors remaining in the radiation damage assessment of the lasers. A test was therefore performed at the Paul Scherrer Institute (PSI), with 330MeV positive pions, on fully packaged Italtel lasers. The rest of this report describes this investigation and compares the damage from pions to that from neutrons, protons and gammas.

# 2. Experiment

## 2.1 Devices and pre-irradiation measurements

Five Italtel/NEC lasers, identical to the devices irradiated previously with neutrons, protons and gammas, were irradiated with pions in this experiment. The devices are labelled 1 to 5 in the following sections. The lasers were the double-channel-planar-buried-heterostructure (DCPBH) multi-quantum-well (MQW) type described in detail in Refs[7,16]. All were supplied with 2m long, pure-silica core (PSC), single-mode fibre pigtails, angle-cleaved at the laser-fibre interface and terminated at the output with FC/PC connectors.

The fibre pigtails are the same as those used in the packaged Italtel devices irradiated with protons, gammas and neutrons (during 1997), but are different to those used in the 1996 neutron tests which used Ge-doped fibre, lensed at the laser end (by chemically etching the core and cladding layers). The change in the fibre type should not affect the radiation damage results in these tests as the length of the fibre pigtail that is exposed to radiation is very short. However, inside the CMS tracker, ~10m of fibre will be exposed to radiation and the overall radiation hardness may be improved by using PSC fibre as it is typically more radiation resistant, in terms of

---

[a] Italtel, Photonic Component Unit, Castelletto, 20019 Settimi Milanese (MI), Italy.

induced attenuation, than Ge-doped fibre[12] (though it should be noted that under particular conditions, such as high dose rate and large doses, Ge-doped fibre can be more rad-hard).

The output power versus input current characteristics (L-I curve) of the lasers measured before irradiation (at ~20°C) are shown in Fig. 1. All the lasers had threshold currents of 8-9mA before irradiation, with a slope-efficiency of 0.046-0.069W/A. The difference in efficiency from device to device is probably due to variations in the laser-fibre alignment and variation in the optical attenuation at the FC/PC connectors.

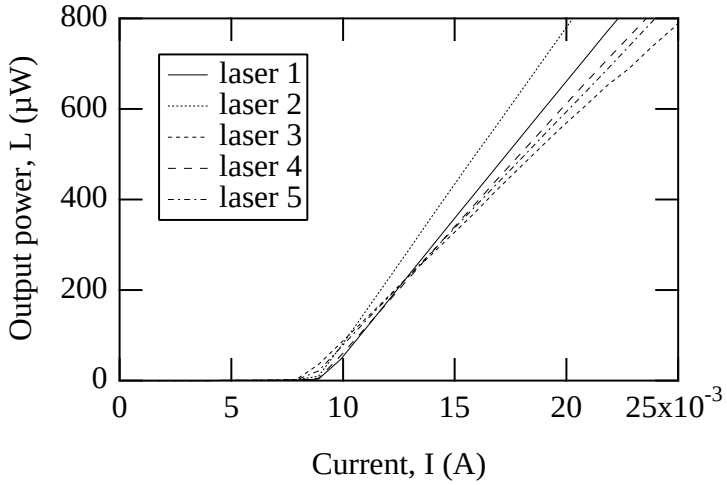


Fig. 1: Laser L-I characteristics before irradiation. Data points measured at 1mA intervals.

## 2.2 Irradiation set-up and dosimetry

The πE-1 pion beamline at PSI has been well characterised by other groups carrying out irradiation tests on solid state detectors for LHC applications[17,18]. In contrast to other tests where the energy of the pion beam was swept over some range, we used a single momentum value of 300MeV/c (i.e. 330MeV energy) in order to reach a sufficiently high fluence. Previous users of the πE-1 facility determined that background levels of proton, neutron and positron contamination are all low enough level to be insignificant in terms of their radiation damage contributions relative to the pion damage.

Samples to be irradiated were arranged, along with dosimetry foils, in a box (a 30cm long, standard 50-slot slide-projector magazine), mounted on a table that can be moved in all three x-y-z directions. The z-axis of the table was first aligned in parallel to the beam direction and then the sample box was aligned in x-y to the beam-centre position by briefly exposing photographic films fixed to the front end of the sample box. The beam profile was then measured at 50mm steps in z-position by using a wire chamber with x-y readout that could be moved horizontally into (or out of) the beam in front of the sample holder. The beam was elliptical, with FWHM increasing along the z-axis from 13 to 25mm in x (horizontal) and 13 to 40mm in y (vertical), as illustrated in Fig. 2. The fitted lines shown in Fig. 2 were obtained using the formula for the width W(z) of a focused beam, along the beam axis[19],

$$W(z) = \sqrt{\left(k_1 + k_2 z + k_3 z^2\right)} \qquad (3)$$

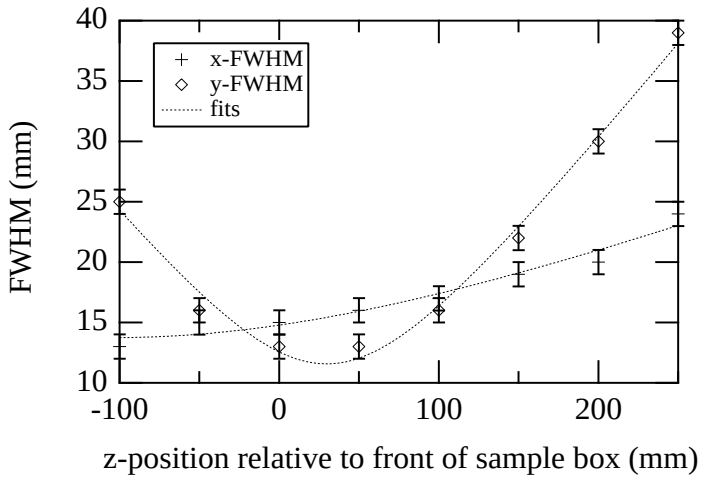


Fig. 2: Beam x- and y-FWHM values measured with a 2-D wire chamber and fitted lines (according to text).

The devices were irradiated for 96 hours at room temperature. Dosimetry was carried out using aluminum foils which become activated by the reaction $^{27}Al(\pi^+, xN)^{24}Na$. The dosimetry foils were placed at various points along the z-axis inside the sample holder, centred on the nominal beam position, and were replaced every 12-15 hours, with activity measurements made within a few hours of removal. The unstable sodium nuclei undergo $\beta^-$-decay with a half-life of 15.1 hours, accompanied by the emission of two photons with energies of 1.37 and 2.75MeV. A Ge-Li detector was used to count the 1.37MeV gammas (with a typical statistical error of ~5%) and the integrated flux was then determined, accounting for both the irradiation time, the time since the end of the exposure, and the GeLi detector position (10cm away) and efficiency (15%). Two or three pieces of foil were used at each position (stacked perpendicular to the beam) in order to achieve a reasonable count rate. No significant difference was measured in the count rate measured in any one of the foils. The beam-time was shared with two other groups whose dosimetry results are also included in this report.

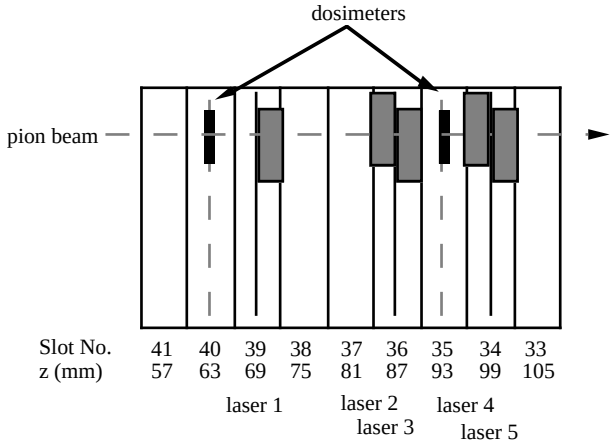


Fig. 3: Schematic layout of devices and dosimeters in the pion beam.

The arrangement of the lasers and dosimetry foils in the sample holder is shown schematically in Fig 3. P-i-n photodiodes were also irradiated further downstream and the results will be reported in a future report. The lasers were mounted back-to-back on PCB cards that slotted into the sample holder box. The lasers were up to a few millimetres away, in the z-direction, from the nearest dosimetry foil. The pion fluence at each laser z-position was therefore calculated by interpolating along the z-direction between dosimeters, along a fitted line as in Fig. 4.

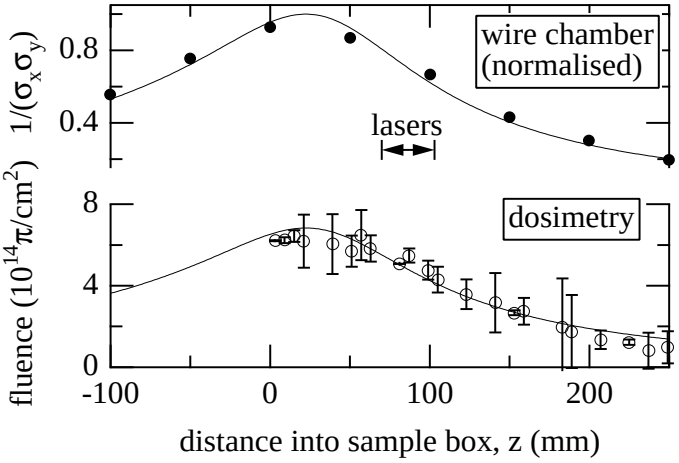


Fig. 4: Fluences measured along sample box in z-direction, compared to normalised beam intensity ($1/\sigma_x\sigma_y$), where $\sigma$ is FWHM/2.35. The lines are a fit to the intensity profile measured with the wire chamber, followed by a fit (of the peak height) to the dosimetry data.

There was a small horizontal offset (±1.5mm) of each device with respect to the nominal beam position, as shown schematically in Fig. 3. The horizontal beam profile was therefore more carefully measured (at slot number 35), to fix the beam position relative to the lasers and dosimetry foils. 7 lots (of 3 pieces) of 2.5mm wide dosimetry foils were arranged to cover the horizontal spread of the beam. The resulting x-profile is shown in Fig. 5, which indicates that the beam was offset by 1.6mm from its nominal horizontal position. The overall similarity of the x-profile with that measured with the x-y chamber confirms that the material upstream (several diamond detector samples) did not significantly modify the beam. The lasers on the upstream side of the PCB cards (devices 2 and 4) were therefore very close to the x-centre of the beam, whereas those on the downstream side (devices 1, 3 and 5) were 3.1mm from the beam centre. The dosimetry was therefore corrected for each laser, taking into account the horizontal offset, using the beam x-FWHM value, beam centre x-position and the x-offset of the particular laser. This added 2.7% to the fluence for the lasers on the upstream sides of the PCB cards and reduced the fluence on the downstream sides by 4.7%. The fluence for the different lasers (devices 1 to 5 respectively) was 5.4, 4.9, 4.6, 4.4 and 4.2 x $10^{14}\pi/cm^2$ (±9% in all cases).

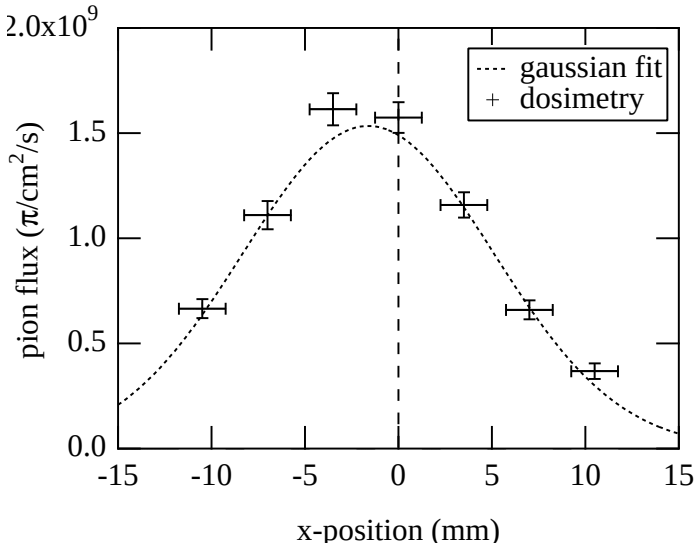


Fig. 5: Horizontal beam profile (looking downstream) at slot number 35 (in front of laser number 4). The beam x-FWHM was found to be 15.8±0.2mm and the beam x-offset was 1.6±0.1mm.

## 2.3 In-situ measurements

During the irradiation and recovery period the laser L-I and V-I (voltage-current) characteristics were monitored at intervals of 30 minutes (increased to one hour during the last 10 days of annealing measurements at PSI). Three of the lasers were biased continuously (typically ~10mA above threshold) and the other two devices were only biased during the L-I measurements, which typically took ~1minute. The unbiased lasers were shorted to ground at other times. The threshold current and slope efficiency were extracted from the measured L-I characteristics, using a line fitted to data for power levels between ~50μA and ~300μA (typically 5 data points). Where the fitted line crosses the x-axis is defined as the threshold current and the efficiency is defined as the gradient of this line. The exclusion of data for higher power levels reduces the systematic error due to the small downward curvature of L-I characteristic - this behaviour is usual in semiconductor lasers and is normally attributed to heating of the junction causing an increase in threshold current[16], though it can also be due to leakage of the input current through the confinement diode structures that surround the active volume[20].

The temperature in the beam area was monitored but not controlled and values between 18°C and 20°C were measured in the beam area during irradiation. The heating of the devices due to the pion beam itself is not likely to have been significant, especially in comparison with the large radiation damage effects measured. After a fluence of ~$5x10^{14}\pi/cm^2$ (averaged across the devices), the lasers were removed from the beam and stored for one month in the beam area, with the same bias and measurement cycles and no modifications to the optical connections. Further measurements of the damage annealing were later continued at CERN using different temperatures between 40 and 80°C.

# 3. Results

## 3.1 Evolution of laser L-I characteristics

The damage due to pion irradiation to the laser L-I characteristics is illustrated in Fig. 6 for laser 1 at different points during the irradiation. The increase in threshold current and loss of efficiency are both clearly visible, as is the good linearity of the device L-I characteristic, even after high fluences.

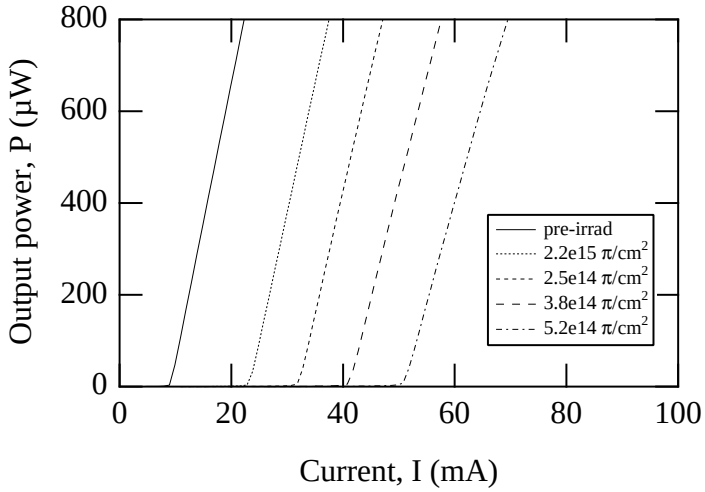


Fig. 6: Change in laser characteristics (in laser 1) due to pion irradiation. Data points were measured at 1mA intervals.

The threshold current increase and efficiency loss are shown for all five devices in Fig. 7 as a function of pion fluence (without any corrections for annealing during the exposure). The data for the biased lasers (1-3) are all in good agreement, whereas there is a large difference in the damage effects in the unbiased devices (4 and 5); laser 4 has almost twice the damage of laser 5 (and lasers 1-3). This anomaly is outside the limits of the dosimetry errors and is not understood. Electrically biasing the devices during irradiation normally decreases the degree of radiation damage by increasing the amount of annealing that takes place during irradiation[7]. This effect is widely known as ‘injection-enhanced annealing’ as observed in other irradiation studies on lasers[21] and LEDs[22], but the magnitude of the enhancement varies in different types of device and semiconductor material. In the earlier irradiation studies the effect of biasing the devices reduced the damage by 29% in proton irradiated devices and 26% in neutron irradiated devices (see Section 4), so it would appear as though the laser 4 is more damaged and laser 5 is less damaged than expected.

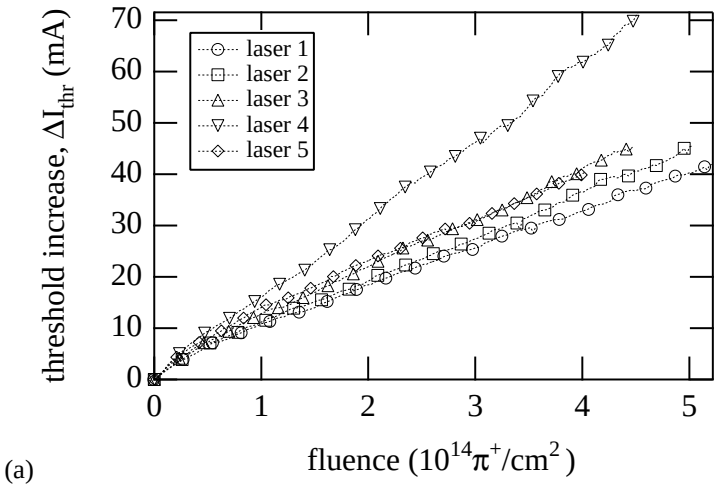


(a)

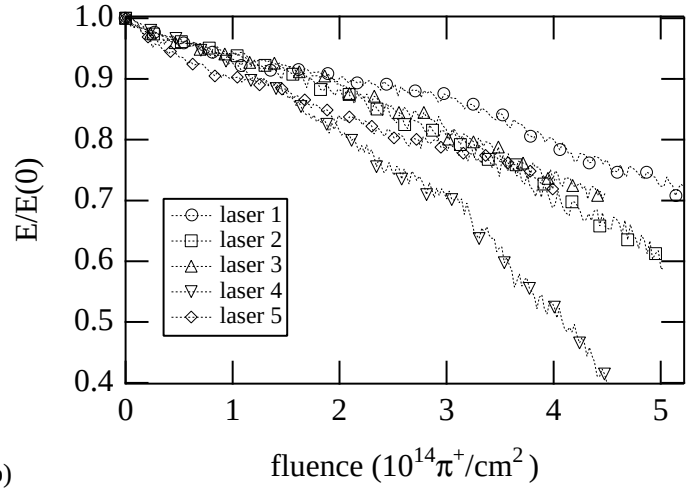


(b)

Fig. 7: Radiation damage to lasers in terms of (a) threshold increase, and (b) efficiency decrease versus pion fluence. Lasers 1-3 were biased 5-10mA above threshold during irradiation and lasers 4 and 5 were short-circuited during irradiation (except during measurements).

The overall threshold shifts and efficiency losses are larger than those observed in (~6MeV) neutron irradiation and similar to those obtained in proton irradiation. The data are compared in more detail in Section 4. However, it should be noted that although the radiation induced changes are large, the fluences reached are higher than those expected for most parts of the CMS tracker (e.g. up to a factor 3 higher than the pion fluence expected at a radius of 20cm - the innermost layer of the silicon tracker); in addition the effect of annealing has also to be taken into account when considering the long irradiation timescales during CMS operation. The radiation induced efficiency loss appears to be tolerable in terms of the CMS analogue link application, and the laser driver circuit for the analogue link is currently specified[23] to track changes in the threshold up to 50-60mA, which should be sufficient when annealing effects are considered along with the radiation damage results, as outlined in the following section.

## 3.4 Annealing of laser damage after irradiation

### 3.4.1 Room temperature

The annealing of the radiation damage to the laser threshold at room temperature (17-21°C) is shown in Fig. 8, for a period of 610 hours following irradiation (which is also included in the figure from -96 < t < 0 hours). Fig. 9 shows the recovery data normalised to the threshold increase measured at the end of the irradiation, which effectively represents the unannealed fraction of defects remaining after time t following irradiation, if the threshold increase is proportional to the defect density as expected. As with the data during irradiation, the results are consistent for all the biased devices (lasers 1-3) with ~35% annealing in 600 hours. The unbiased lasers (4 and 5) have different behaviour; laser 5 is similar to the biased devices but laser 4 has 5-10% greater annealing overall.

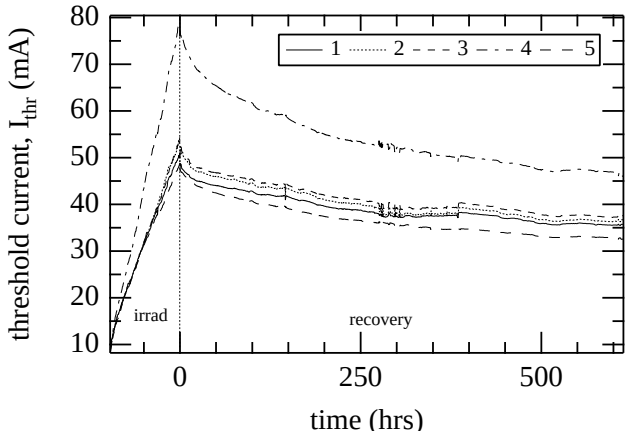


Fig. 8: Irradiation and recovery data for laser threshold current.

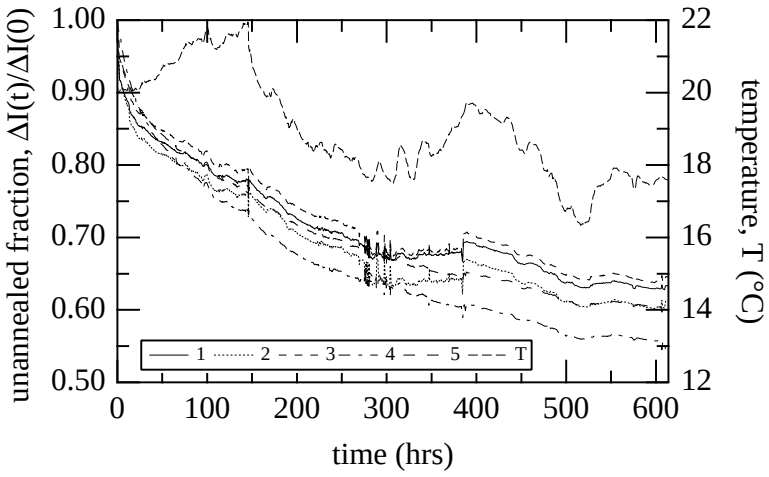


Fig. 9: Annealing of the threshold damage at room temperature. The threshold shift has been normalised to the value at the end of the irradiation so that the plot shows the fraction of unannealed defects.

The annealing data is relatively noisy mainly due to large temperature fluctuations, 16-22°C (shown in Fig. 9) during the recovery period compared to 18-20°C during irradiation. The efficiency data is not included as the devices had to be moved after irradiation and this disturbance altered the amount of light transmitted in the fibre. This should not normally present a problem but the pure-silica mode fibre pigtails were not single-moded at 1310nm (the fibres were actually optimised for 1550nm operation), therefore changes in the optical coupling (typically ±10%) can occur when the fibre is displaced, affecting the efficiency measurement but not the threshold measurement.

### 3.4.1 Accelerated annealing at higher temperatures

The annealing measurements were restarted two months after irradiation, using an oven to investigate the acceleration of the annealing at elevated temperatures**.** The lasers were monitored as in the previous irradiation/recovery periods at consecutive temperature steps of 40°C, 60°C and 80°C. The duration of each temperature step was approximately 260 hours. Results for the annealing of the laser threshold current damage (normalised to the value measured at the end of the irradiation) are shown in Fig. 10. As the threshold current varies exponentially with temperature, all the data measured at 40°C and 60°C were scaled to 20°C using measurements taken at 20°C before and after each higher temperature step. For the annealing step at 80°C, the laser L-I characteristics were not sufficiently linear to extract a reliable threshold current value and the annealing data was therefore obtained by remeasuring the characteristics every 20-24 hours at 20°C(±0.2°C).

The measurements indicate a maximum of 65% annealing in the recovery time/temperature range tested. It is encouraging to observe that no ‘anti-annealing’ took place in the lasers, in contrast to, for example, the further increase in radiation damage that occurs in highly irradiated silicon detectors during annealing (following irradiation) when stored at temperatures above 0°C[24]. Further measurements on a larger sample of devices (split into groups annealed at separate temperatures) are planned in order to precisely measure the activation energies associated with the annealing behaviour. With knowledge of the activation energy spectrum, it would be possible to predict more precisely the recovery dynamics at different temperatures. In addition a direct measurement of annealing at -10°C is planned to determine the recovery rate at the temperature expected inside the silicon/pixel regions of the CMS tracker.

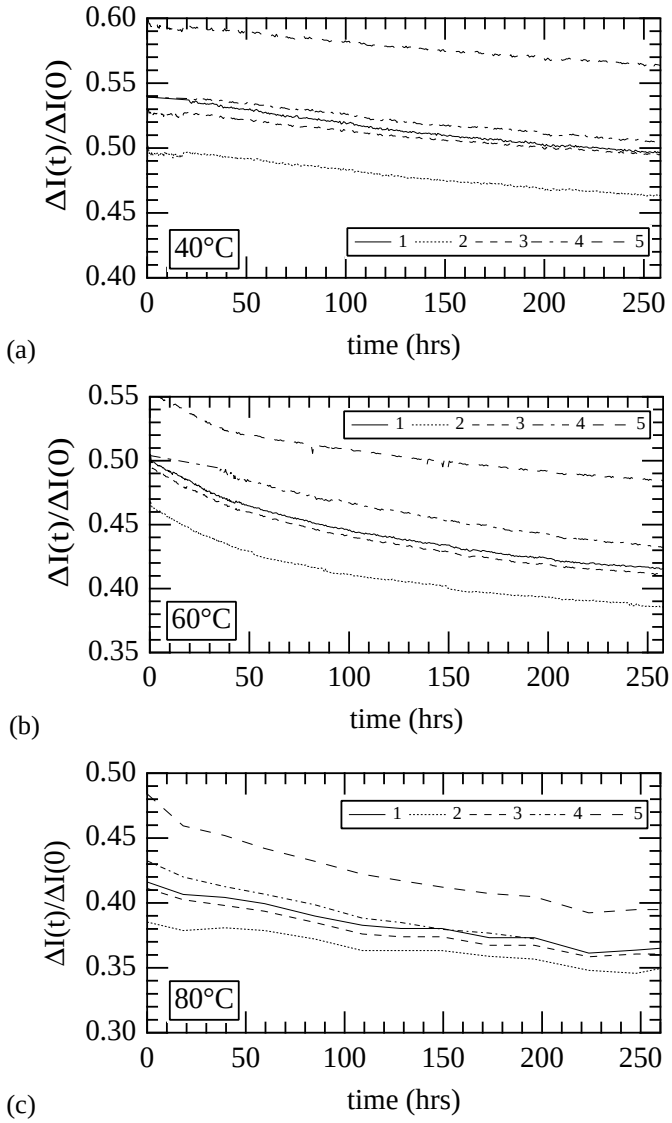


Fig. 10: Annealing of threshold current damage at (a) 40°C, (b) 60°C, and (c) 80°C, corrected to correspond to the threshold values at 20°C.

## 4. Comparison of damage in pion, neutron and proton tests

Devices of the same type (Italtel fully packaged lasers) have now been irradiated with pion, proton, neutron and gamma sources. Gamma damage will not be discussed further as the effects were not significant compared to hadron damage, for dose/fluence levels expected during LHC operation[8].

The data from pion irradiation can be compared directly with that from neutron irradiation since the irradiation periods were the same (96 hours) and no corrections have to be applied for the annealing that took place during the irradiation. To make a comparison between 330MeV pion and 24GeV proton damage, a correction has to be applied to the proton data. The proton irradiation was carried out over 10.5 hours with a fluence of $3.5 \times 10^{14} p/cm^2$. Annealing data were measured for 350 hours following irradiation[8]. Given the linear dependence of damage with fluence, it can be assumed that for an irradiation to a different fluence $\Phi$ in the

same period of 10.5 hours, the damage during irradiation (and the following 350 hours) would be the same as for the actual proton damage data multiplied by a factor ($\Phi/3.5x10^{14}p/cm^2$). A reasonable comparison between the 96 hour pion and the 10.5 hour proton irradiation can therefore be made if the effects of 9 consecutive proton irradiations are calculated (i.e. one 10.5 hour irradiation plus 85.5 hours of recovery, plus another 10.5 hour irradiation plus 75 hours of recovery, etc. to result in an effective irradiation time of 94.5 hours).

Fig. 11 compares the threshold damage from pion, neutron and proton irradiation in biased and unbiased lasers. In the biased devices, the laser current was typically 5-10mA above threshold during the irradiation. The neutron irradiation tests used 8 biased and 2 unbiased lasers and the proton test included 3 biased and 2 unbiased lasers. The 330MeV pions are 3.9±0.8 more damaging than ~6MeV neutrons in biased lasers and 3.7±1.1 more damaging in unbiased lasers (the larger uncertainty being due to the greater difference in the damage in the two unbiased lasers exposed to pions). Pion damage is very similar to the predicted level of proton damage, giving relative $\pi$/p damage factors of 1.2±0.3 for the unbiased devices, and 1.2±0.2 for the biased devices.

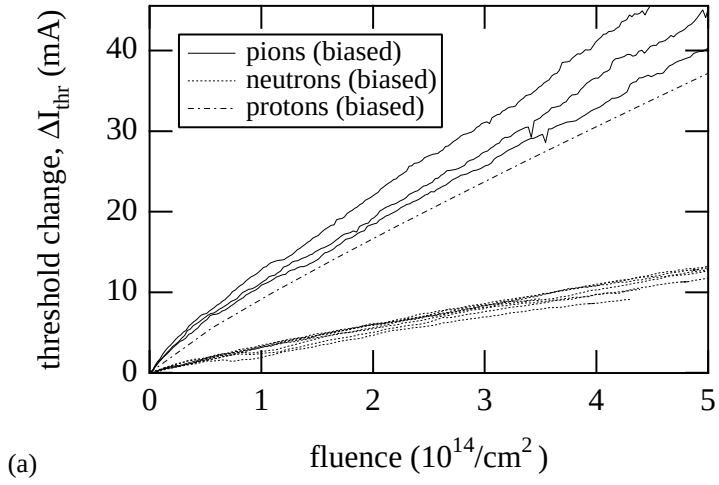


(a)

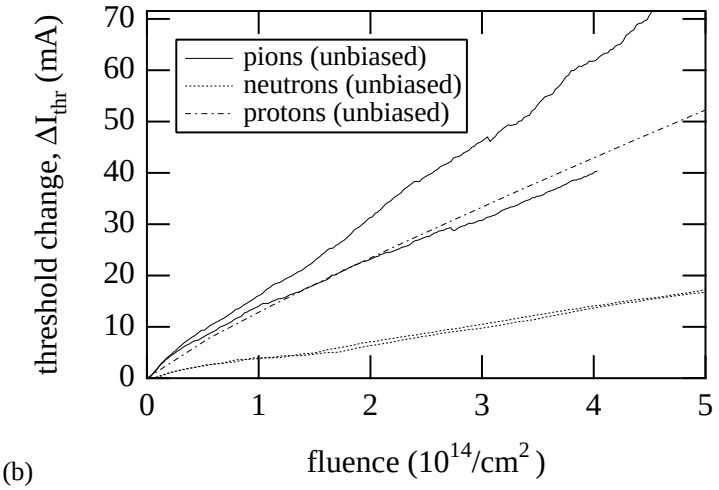


(b)

Fig. 11: Threshold increase comparison between neutron, proton and pion irradiated lasers, (a) for biased devices and (b) for unbiased devices. The proton damage data is extrapolated to an irradiation period of 95 hours and total fluence of $5x10^{14}p/cm^2$.

It should be noted that, in both proton and pion irradiations, the devices were oriented with the active layer perpendicular to the incident beam. Although, in our measurements of 6MeV neutron damage, no significant effect has been observed for lasers inclined at different angles to the incident neutrons, recent measurements on GaAs lasers with 300MeV protons indicate up to 50% increase[25] in damage when the irradiation direction is parallel to the active layers rather than perpendicular. It is therefore likely that the level of damage will be different for devices situated at different points in the tracker despite receiving similar particle fluences and this effect will be tested for the CMS tracker optical link components in future irradiation tests using high energy beams.

It is interesting that the large difference observed between the effects of ~6MeV neutrons and those due to 24GeV proton and 300MeV/c pions is qualitatively similar to that observed in GaAs detectors, where the ratio is 1:3.1:3.8 for 1MeV neutrons, 24GeV protons and 300MeV/c pions respectively[13]. In contrast, the damage ratios are very similar in silicon detectors (1:0.93:0.93)[14]. The explanation for this difference in ratios between Si and GaAs (and we assume it also applies to the lasers) is related the masses of the constituent elements and the fraction of the kinetic energy of recoiling atoms/nucelei that is dissipated in further atomic displacement, the non-ionising energy loss (NIEL), as opposed to generating ionisation[15,26,27]. The argument for greater damage in GaAs and InGaAsP with higher energy incident particles such as in the pion and protons irradiation tests relative to ~1MeV neutron damage is outlined in the Appendix. More detailed calculations of NIEL (and Monte-Carlo simulations of the basic interactions) are necessary, that should also include the laser geometry, the different (elastic and inelastic) interaction cross-sections and the full spectra of recoil energies, to check, first of all, whether the observed damage in lasers is proportional to NIEL, and then to make predictions for the radiation damage expected during CMS operation.

## 5. Conclusion

In the silicon microstrip and pixel parts of the CMS Tracker the radiation flux will be dominated by pions with ~300MeV energy. We have measured the radiation damage effects due to 330MeV (positive) pions on lasers for use in the analogue optical readout links, with fluences between 4.2 and $5.4 \times 10^{14} \pi/cm^2$. Five devices were irradiated at room temperature, three biased continuously and the other two biased only during measurement of the laser L-I characteristics.

The laser threshold current increased by 32-40mA in the biased devices, (after $4 \times 10^{14} \pi/cm^2$) compared with 62mA in one unbiased device and 40mA in the other. In terms of output efficiency, pion damage caused 20-30% loss (after $4 \times 10^{14} \pi/cm^2$) in the biased devices and 50% and 30% in the two unbiased devices. The difference in the level of damage in the two unbiased lasers is not understood though this is not of great concern since devices will be irradiated under bias in the CMS Tracker. The annealing of the threshold current was monitored after irradiation, with 30-40% of the damage annealing at room temperature in 600 hours following irradiation. Further measurements of the annealing were made at 40°C, 60°C and 80°C (260 hours at each step) and a further 25-35% of the damage was recovered by the end of this accelerated annealing test. No anti-annealing was observed.

The threshold damage results during pion irradiation have been compared with data from earlier neutron and proton irradiation tests on the same type of laser. 330MeV pions are 1.2 times more damaging than 24GeV protons and 3.8 times worse than ~6MeV neutrons. Overall there is no significant difference between the relative damage ratios for biased and unbiased lasers, except for a greater level of uncertainty in the unbiased devices. It is likely that the difference in damage is linked to the level of non-ionising energy loss (NIEL), as found in other irradiated semiconductor devices and work is underway to calculate the NIEL for the lasers.

The results of this test are promising in terms of long-term link operation inside the CMS tracker. The latest specifications for the laser driver electronics allow for threshold increases up to 50-60mA, which are unlikely to occur over a long term irradiation such as inside the CMS tracker, where annealing during the LHC running and shutdown periods will suppress the build-up of radiation damage effects. To allow the optical link specifications to contain some safety margin, further tests are required to accurately determine the activation energy for the recovery, or to make a direct measurement of the annealing rate at -10°C (the foreseen temperature inside the silicon and pixel elements of the CMS tracker). In addition, further irradiation tests are planned to measure the effect of incident particle direction on the radiation damage in the lasers for high energy hadrons.

## Acknowledgements

We wish to thank Bernard Cornet and Loic Baumard for preparating the test hardware; Francois Lemeilleur, Maurice Glaser and Mika Huhtinen of CERN for very useful advice; Kurt Gabathuler of PSI for arranging the pion irradiation, and the Vienna and Dortmund groups for their assistance during the irradiation test and for sharing the dosimetry measurements.

## Appendix

### Non-ionising energy loss of recoiling atoms in different semiconductors

The non-ionising energy loss (NIEL)[15] fraction is larger for heavier atoms of a given recoil energy, as illustrated in Fig. A.1 which shows the amount of recoil energy that is non-ionising, i.e. is lost in generatig further atomic displacements, in Si, GaAs and InGaAsP material. The plots were generated using the Lindhard theory for stopping power[26], applying the formulae given in Ref.[27], making the appropriate averaging corrections for the compound GaAs and InGaAsP material.

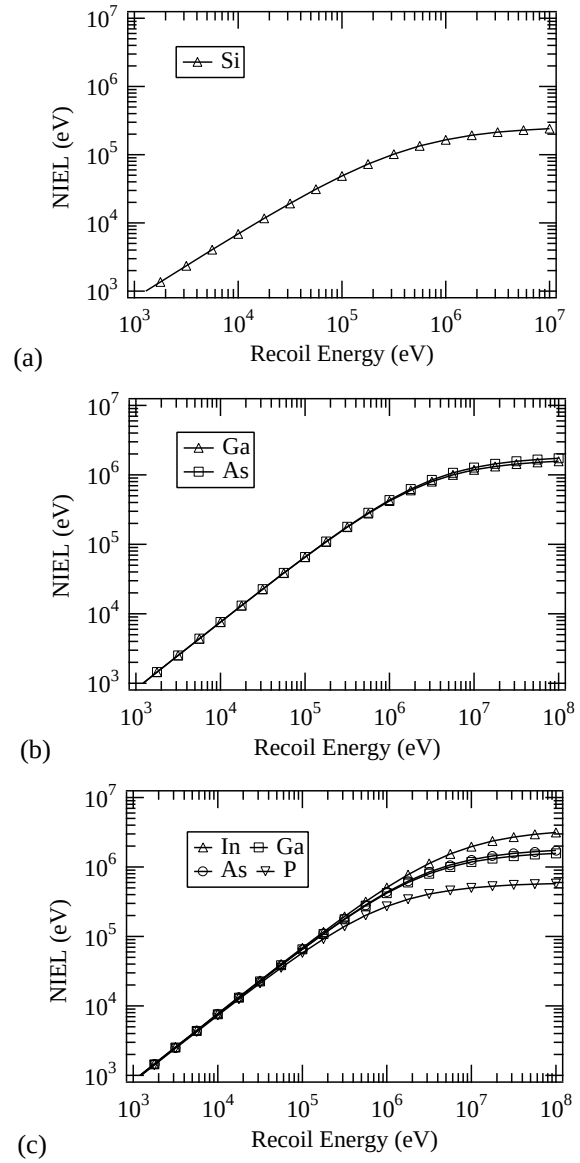


Fig. A.1: Non-ionising energy loss of different atoms in different bulk materials, as a function of the recoil energy of the atom after being struck by an incident high energy particle. (a) Si recoils in Si, (b) Ga and As recoils in GaAs, and (c) In, Ga, As and P recoils in InGaAsP laser material.

The maximum NIEL of a recoiling Si atom in Si bulk material is found to be ~300keV, compared to a maximum value of ~2MeV for Ga in GaAs bulk material, and ~3MeV for In in InGaAsP. 1MeV neutrons can provide a recoil energy up to 130keV in silicon in an elastic collision, of which 100keV is deposited as NIEL. This is already close to the limit of maximum NIEL per recoil and higher energy incident particles are therefore not expected to cause much more damage in silicon, even though recoiling nuclear fragments (albeit with atomic number much less than 28 in some cases) can have up to ~100MeV energy in 24GeV proton-nucleon inelastic collisions. In the case of GaAs, the maximum recoil energy from 1MeV neutrons is ~60keV, typically dissipating 40keV of this energy in further atomic displacements. Since the NIEL in GaAs (and InGaAsP) is up to several MeV per recoil, it is clear that higher energy protons and pions will generate more damage per recoiling atom than a 1MeV neutron.

## References


[1] F. Vasey et al, Proceedings of IEEE Nuclear Science Symposium, 1997, to be published in IEEE Trans. Nucl. Sci., June 98.

[2] V. Arbet-Engels et al., Proceedings of 7th Pisa Meeting on Advanced Detectors, to be published in Nucl. Instr. and Meth. A.

[3] G. Hall, Nucl. Instr. and Meth. A.386 p.132 (1997).

[4] CMS Tracker Technical Design Report (1998). Note that uncertainties in the fluence values may be at the level of 50%.

[5] J. E. Gover and J. R. Srour., "Basic Radiation Effects in Nuclear Power Electronics Technology", Sandia Laboratory Report, SAND85-0776 (1985).

[6] C. E. Barnes and J. J. Wiczer, "Radiation Effects in Optoelectronic Devices", Sandia Laboratory Report, SAND84-0771 (1984).

[7] K. Gill et al., CMS Technical Note 1997/044.

[8] K. Gill et al., Proceedings of Radiations and their Effects on Devices and Systems Conference (RADECS) 1997.

[9] J. Troska et al, CMS Technical Note 1997/102.

[10] K. Gill et al., Proceedings of Second and Third Workshops on Electronics for LHC Experiments 1996 and 1997.

[11] J. Batten et al., Proceedings of Data Workshop, Radiations and their Effects on Devices and Systems Conference (RADECS) 1997.

[12] K.Gill et al., J.Non-Cryst. Solids 216 p. 129 (1997).

[13] A. Chilingarov et al., Nucl. Instr. and Meth. A.395 p.35 (1997).

[14] S. J. Bates et al., Nucl. Instr. and Meth. A.379 p.116 (1996).

[15] G. P. Summers et al., IEEE Trans. Nucl. Sci., vol.35, p.1221 (1988).

[16] G. P. Agrawal and N. K. Dutta. “Semiconductor lasers”, 2nd Edition, Van Nostrand Reinhold, New York (1993).

[17] P. Aarnio et al., Nucl. Instr. and Meth. A.360 p.521 (1995).

[18] C. Furetta et al., Nucl. Phys. B (Proc. Suppl.) 44 p. 503 (1995).

[19] M. Reiser, “Theory and design of charged particle beams”, John Wiley & Sons, New York (1994).

[20] P. D. Wright et al., J. Appl. Phys., Vol. 53(3), p. 1364 (1982).

[21] B. D. Evans et al., IEEE Trans. Nucl. Sci., vol.40, p.1645, (1993).

[22] R. H. Rose and C. E. Barnes, J. Appl. Phys., Vol. 53(3), p. 1772 (1982).

[23] F. Vasey. CMS Tracker Optical Readout Link Specification (draft).

[24] A. Holmes-Seidle et al., Nucl. Inst. and Meth. A 339 (1994).

[25] Y. F. Zhao et al., IEEE Trans. Nucl. Sci., vol.44, No. 6, p.1898 (1997).

[26] J. Lindhard et al., Mat. Fys. Medd. K. Dan. Vidensk. Selsk. 33, p. 1 (1963).

[27] M. J. Norgett et al., Nucl. Eng. and Des., 33, p. 50 (1975).